

Abstract

For Presentation at
The University of Alabama in Huntsville
October 17, 2008

A Brief Introduction to the Theory of Friction Stir Welding

By Arthur C. Nunes, Jr
Marshall Space Flight Center
Materials and Processes Laboratory, EM30
Huntsville, AL 35812

Friction stir welding (FSW) is a solid state welding process invented in 1991 at The Welding Institute in the United Kingdom. A weld is made in the FSW process by translating a rotating pin along a weld seam so as to stir the sides of the seam together. FSW avoids deleterious effects inherent in melting and is already an important welding process for the aerospace industry, where welds of optimal quality are demanded. The structure of welds determines weld properties. The structure of friction stir welds is determined by the flow field in the weld metal in the vicinity of the weld tool. A simple kinematic model of the FSW flow field developed at Marshall Space Flight Center, which enables the basic features of FSW microstructure to be understood and related to weld process parameters and tool design, is explained.



A Brief Introduction to the Theory of Friction Stir Welding

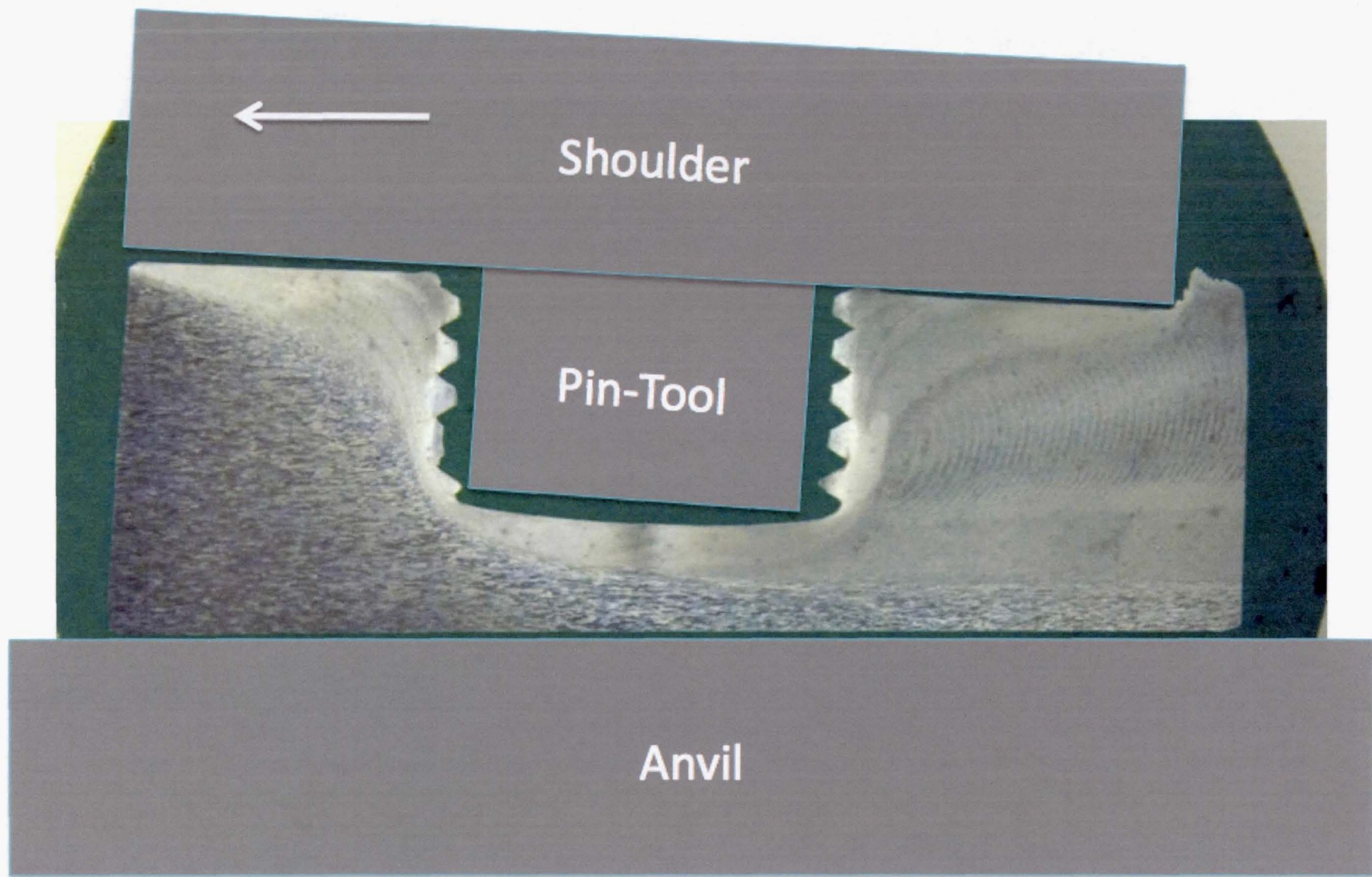
Arthur C. Nunes, Jr.

Metals Engineering Branch
Marshall Space Flight Center

Introduction

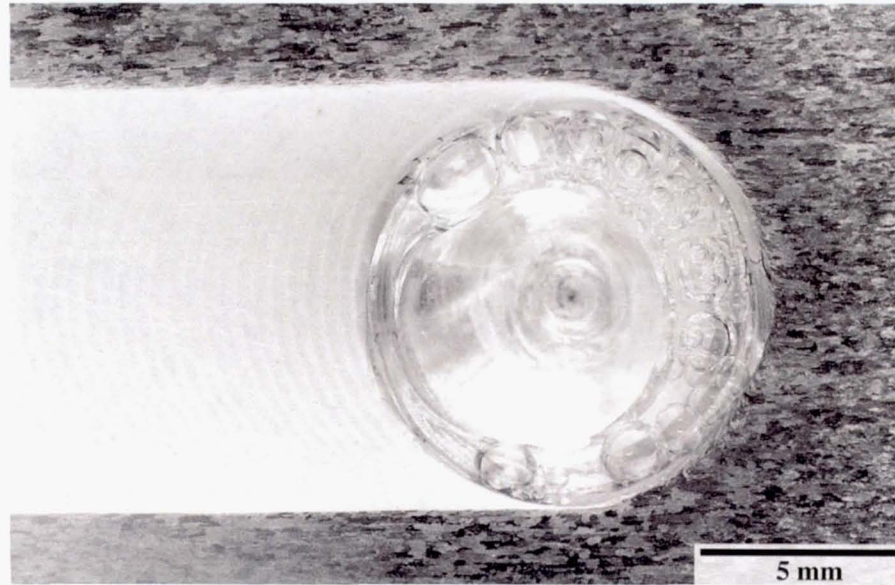
Friction stir welding

- **Is a solid-state seam welding process. Melting does not normally occur. Welding occurs automatically upon placing clean metal in contact.**
- **Was invented in 1991 at The Welding Institute, Cambridge, England (GB Patent Application No. 9125978.8, 6 December 1991).**
- **Avoids melting problems inherent in fusion welding: loss of strengthening structure in residual cast weld metal component; disturbance of dispersed strengthening phases (MMCs); safety issues (heat sources, spatter, molten metal); precision issues (wide fusion penetration variation due to Marangoni circulations); contamination issues (metal vapor may coat optics); etc.**



Basic friction stir welding configuration

Longitudinal section courtesy of J.C. McClure/University of Texas at El Paso



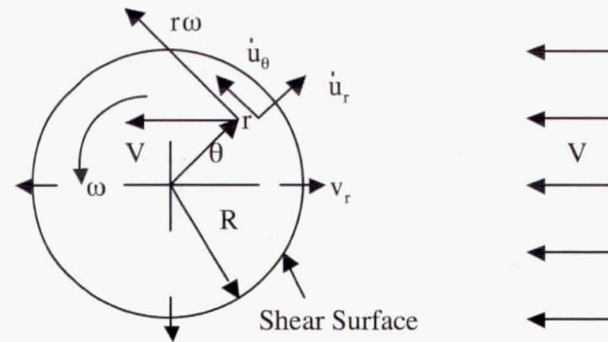
Plan view mid-sectional macrostructure of FSW in 0.317 inch thick 2219-T87 aluminum alloy plate. The pin-tool has been removed and replaced with bubble-filled mounting medium. Rotation is in the counterclockwise direction. The spindle speed was 220 RPM and the travel speed 3.5 inches per minute.

Shear surface, rotating plug model, and wiping transfer mechanism

- Shear occurs at a “discontinuity” in velocity between a plug of metal attached to the pin-tool and the weld metal bulk.
- The forward part of the moving shear surface picks up weld metal, which is rotated (wiped) around the tool in the rotating plug, and left behind as the tool moves on.

Planar Flow Patterns

Mathematical implementation
of rotating plug model



Velocity field of metal in rotating plug (relative to pin-tool) is taken to be a superposition of two fields: 1) rotating cylinder and 2) uniform translation.

$$\mathbf{v} = \frac{dr}{dt} \hat{u}_r + r \frac{d\theta}{dt} \hat{u}_\theta = (v_r - V \cos \theta) \hat{u}_r + (r\omega + V \sin \theta) \hat{u}_\theta$$

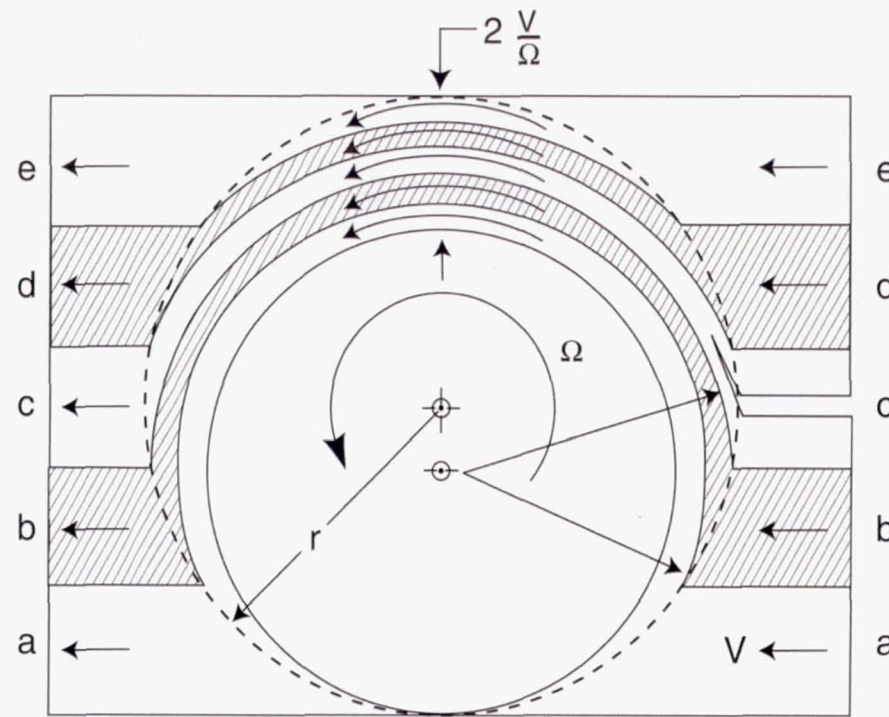
Trajectory of weld metal element inside plug is then:

$$dr = r \left(\frac{\frac{v_r}{V} - \cos \theta}{\frac{r\omega}{V} + \sin \theta} \right) d\theta$$

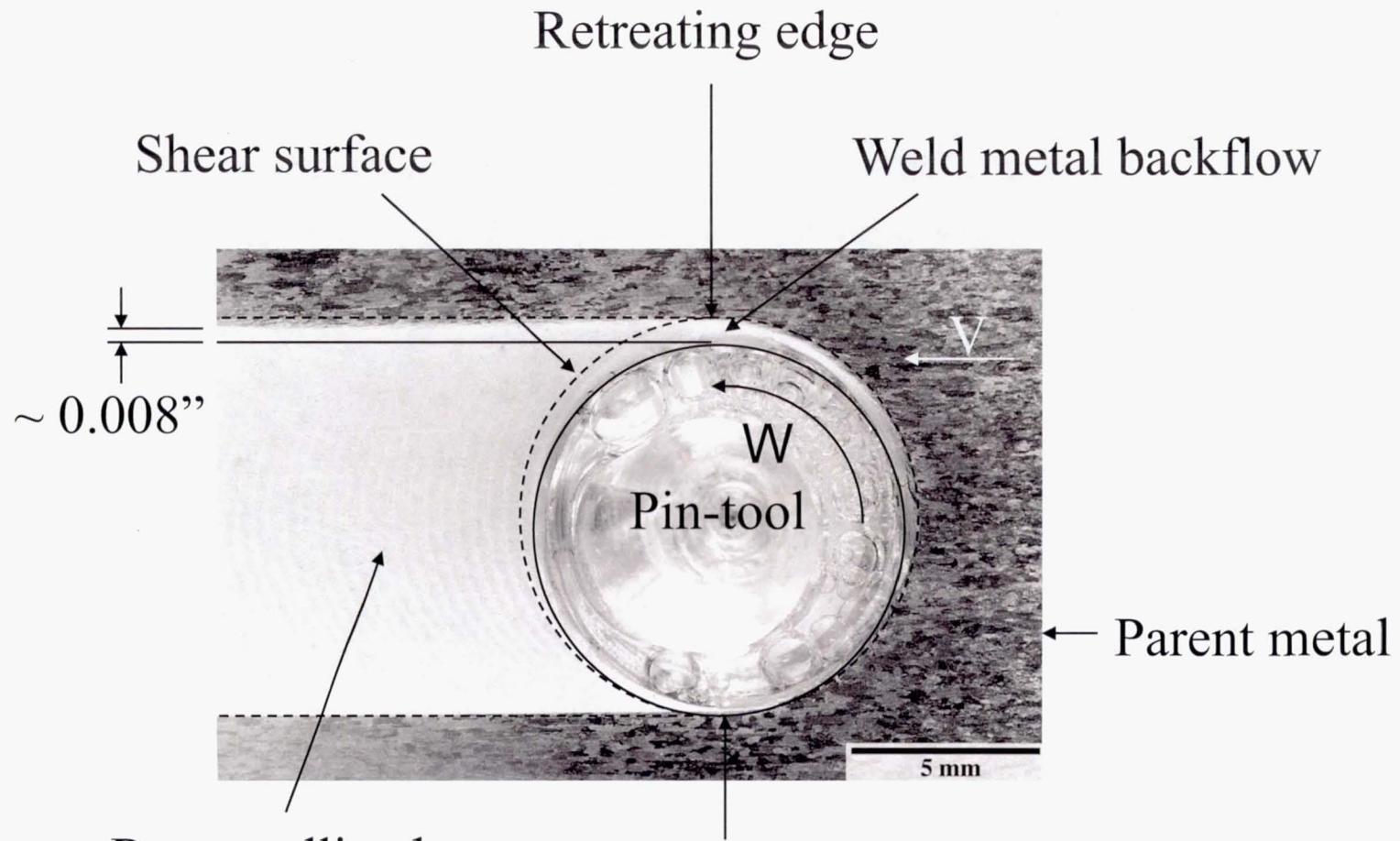
If $v_r \ll V$ and $r\omega \gg V$,

$$dr \approx -\frac{V}{\omega} d \sin \theta$$

In this case the maximum depth is $\Delta r_{\max} \approx -\frac{2V}{\omega}$ on the retreating edge. If the shear surface radius is constant, there is no lateral (y) displacement at exit from the tool.



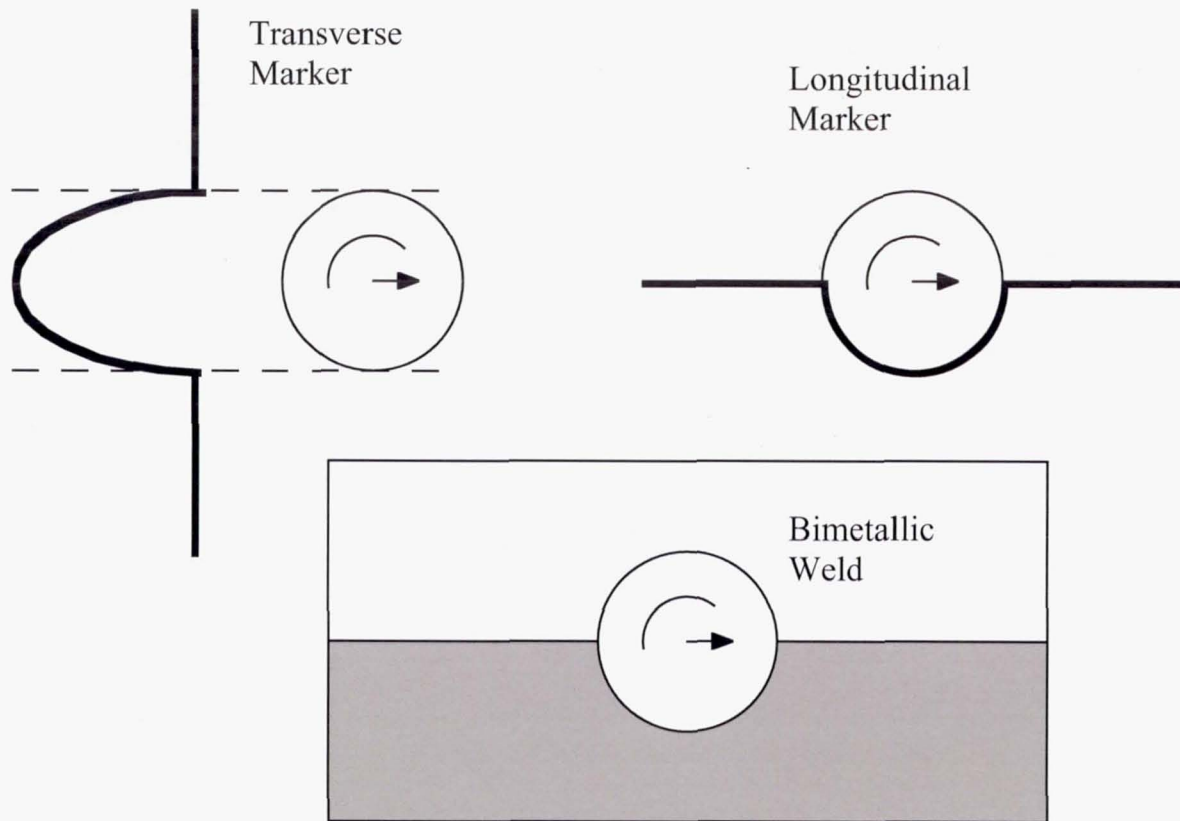
Two-dimensional planar "wiping" flow streamlines for a FSW flow field. The width of the pattern has been greatly exaggerated to reveal the structure more clearly. In the typical FSW case the flow around the tool takes place within a thin sliver of rotating metal just beneath the shear surface



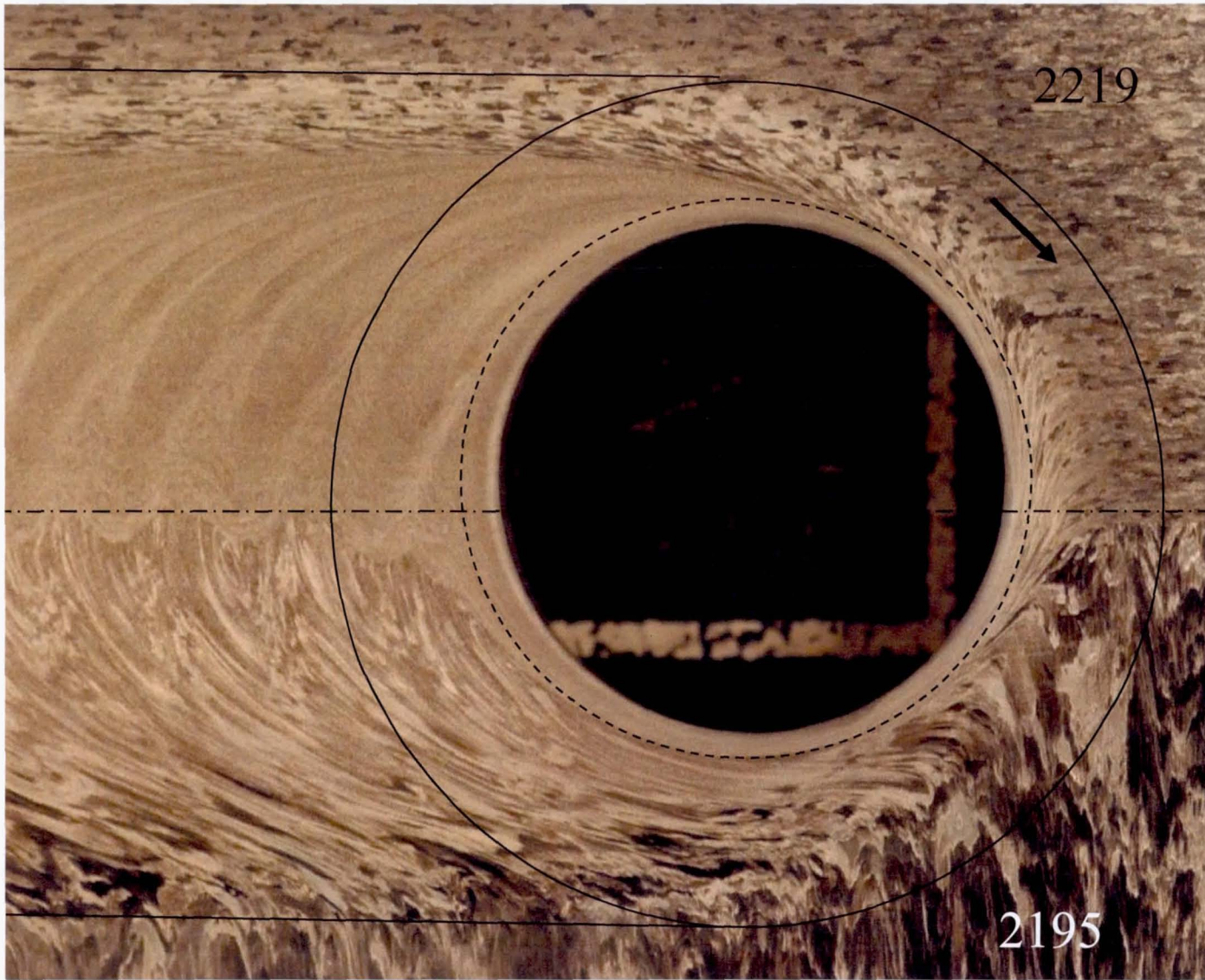
Recrystallized
weld metal
(Note banding)

Advancing edge

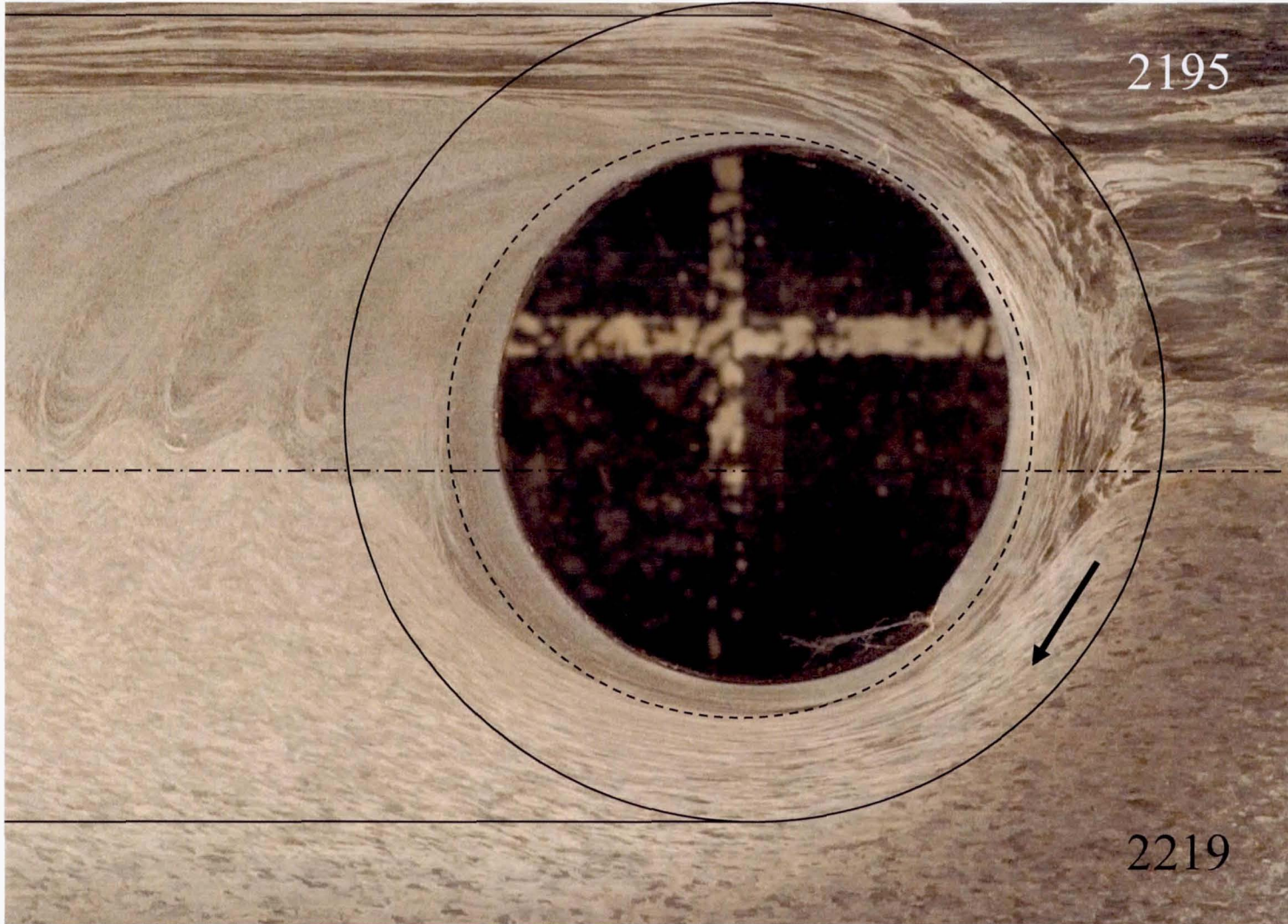
$$2 \frac{V}{\Omega} = 2 \frac{[3.5 \text{ in / min}]}{[2\pi \text{ rad / rev}][220 \text{ rev / min}]} \approx 0.005''$$



PLANAR MARKER PATTERNS DUE TO
TRANSLATING, ROTATING FIELD

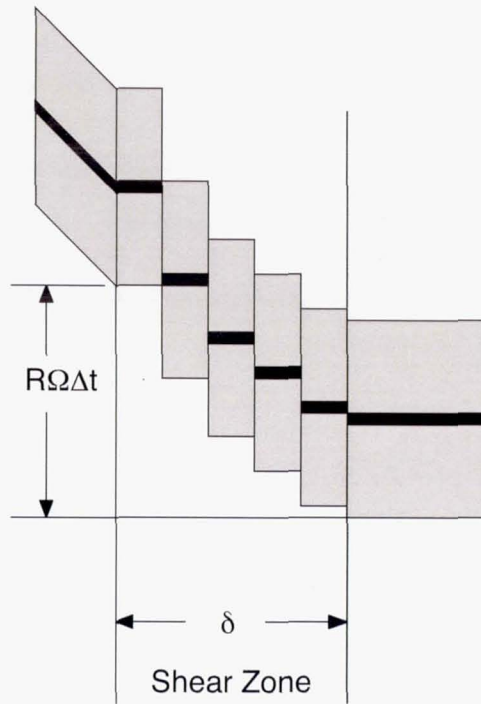


Courtesy of G. Bjorkman/Lockheed Martin



Courtesy of G. Bjorkman/Lockheed Martin

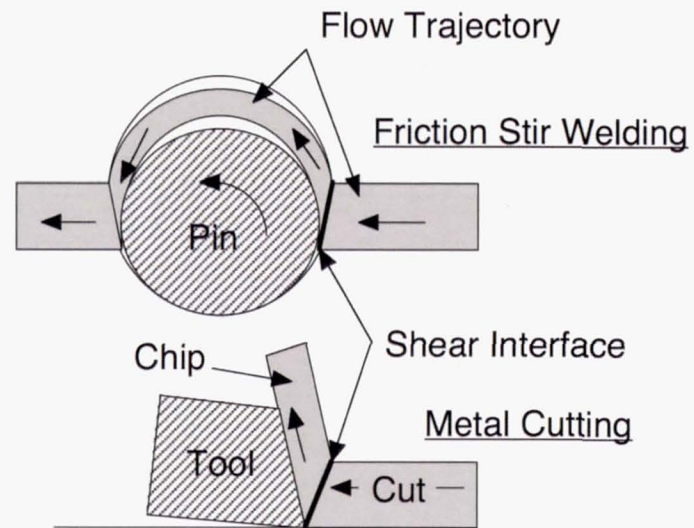
Strain Rates



Shear strain rate
in friction stir welding
is comparable to that of
metal cutting (10^3 to 10^5 sec^{-1}).

$$\frac{d\gamma}{dt} = \frac{\Delta\gamma}{\Delta t} = \frac{\left(\frac{R\Omega\Delta t}{\delta}\right)}{(\Delta t)} = \frac{R\Omega}{\delta} \sim \frac{[0.19\text{inches}] \left[2\pi \frac{\text{rad}}{\text{rev}} \cdot 220\text{RPM} \cdot \frac{1 \text{ min}}{60 \text{ sec}}\right]}{[0.0005\text{inches}]} \sim 0.8 \times 10^4 \text{ sec}^{-1}$$

Comparison of friction stir welding and metal cutting



Low-cost manufacturing process for nanostructured metals and alloys

Travis L. Brown, Srinivasan Swaminathan, Srinivasan Chandrasekar,
W. Dale Compton, Alexander H. King, and Kevin P. Trumble
Schools of Engineering, Purdue University, West Lafayette, Indiana
47907-1287

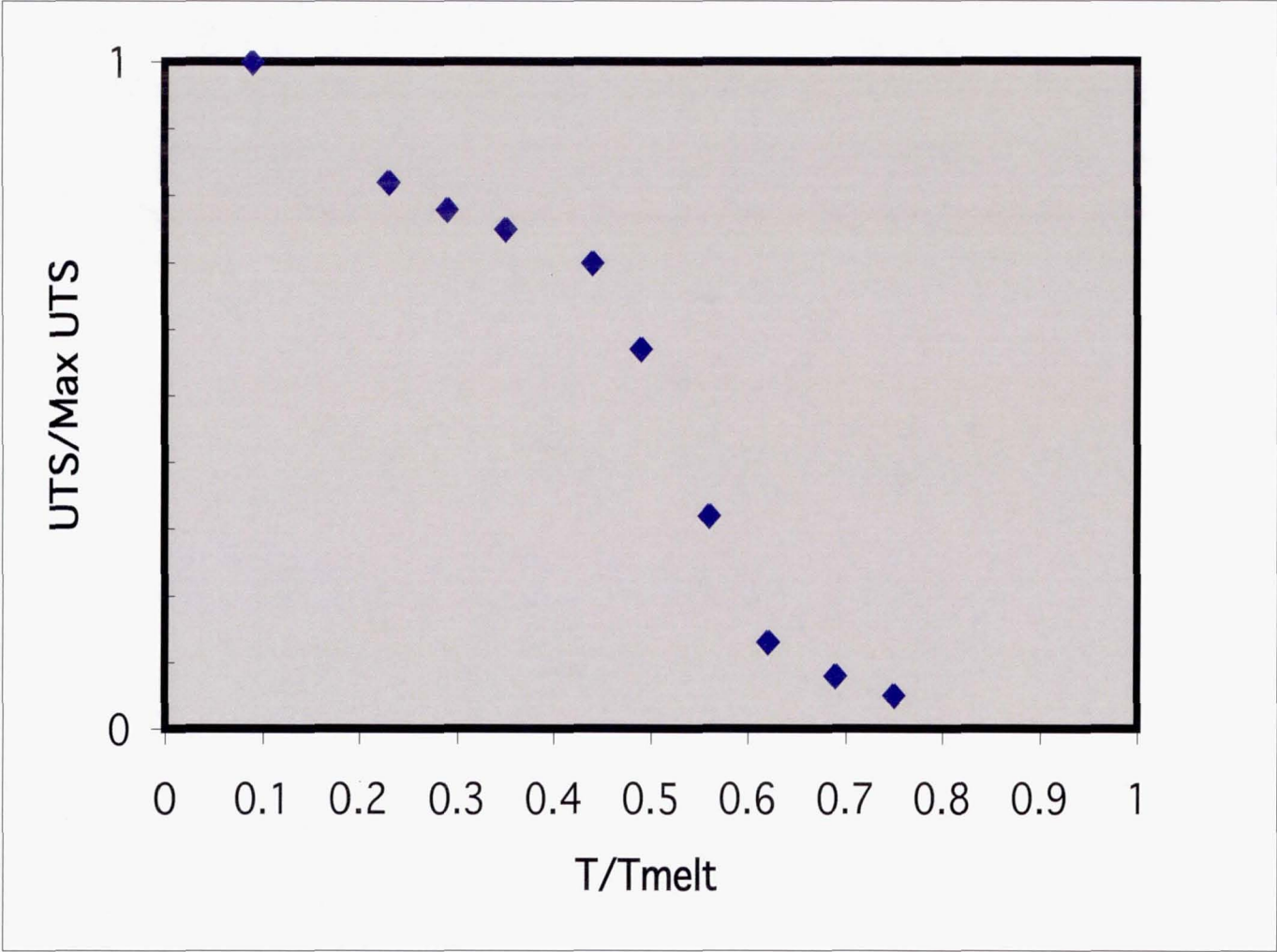
Journal of Materials Research 17 (10) (2002). 2484-2482

In spite of their interesting properties, nanostructured materials have found limited uses because of the cost of preparation and the limited range of materials that can be synthesized. It has been shown that most of these limitations can be overcome by subjecting a material to large-scale deformation, as occurs during common machining operations. The chips produced during lathe machining of a variety of pure metals, steels, and other alloys are shown to be nanostructured with **grain (crystal) sizes between 100 and 800 nm**. The hardness of the chips is found to be significantly greater than that of the bulk material.



Typical friction stir shear produced grains ~ 10,000 nm.

Flow Stresses



Viscous vs. plastic flow models

- Plastic metal flow is less sensitive to strain rate.
- Metals are subject to shear instabilities (inhomogeneities) as denoted on processing maps.

Local rearrangement mechanism (viscous flow)

$$\tau \approx \left(\frac{kT e^{\frac{E}{kT}}}{nv\Delta\gamma} \right) \dot{\gamma}$$

k = Boltzmann's Constant
T = Absolute temperature
E = Activation energy of process
 $\Delta\gamma$ = Shear strain per unit activation
n = Number of activation elements per unit volume
v = Oscillation rate of activation element

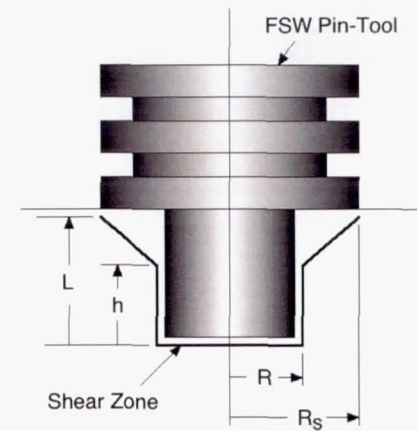
Dislocation slip mechanism (plastic flow)

$$\tau \approx \frac{E}{v} - \frac{kT}{v} \ln \left(\frac{n\Delta\gamma v}{2\dot{\gamma}} \right)$$

k = Boltzmann's Constant
T = Absolute temperature
E = Activation energy of process
v = Activation volume for process
 $\Delta\gamma$ = Shear strain per unit activation
n = Number of activation elements per unit volume
v = Oscillation rate of activation element

A.P. Reynolds and Wei Tang, "Alloy, Tool Geometry, and Process Parameter Effects on Friction Stir Weld Energies and Resultant FSW Joint Properties," *Friction Stir Welding and Processing*, ed. K.V. Jata et al. (Warrendale, PA: The Minerals, Metals & Materials Society, 2001) 15-23.

Tool Configuration	R_s (mm)	R (mm)	L (mm)
1	12.5	5	8.1
2	12.5	4	8.1
3	12.5	6	8.1
4	10.0	5	8.1
5	15.0	5	8.1



$$M = 2\pi R^3 \tau \left\{ \frac{1}{3} + \frac{h}{R} + \sqrt{\left(\frac{L-h}{R}\right)^2 + \left(\frac{R_s-R}{R}\right)^2} \left(1 + \left(\frac{R_s-R}{R}\right) + \frac{1}{3} \left(\frac{R_s-R}{R}\right)^2\right) \right\}$$

$$\frac{h}{L} = 1 - \frac{\frac{R}{L}}{\left[1 + \frac{1}{3} \left(\frac{R_s-R}{R}\right)\right]}$$

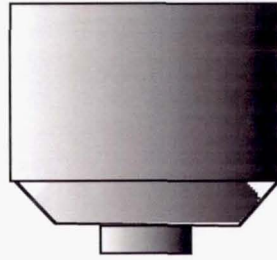
Table I. Effect of Friction Stir Welding Tool Configuration on Power Requirement. Percent error in the computed value in parenthesis next to compared values.

Tool Configuration	Power Requirement (watts)					
	240 RPM/1.3 mm/sec $\tau = 2.01$ ksi*		240 RPM/2.4 mm/sec $\tau = 2.18$ ksi*		390 RPM/3.3mm/sec $\tau = 1.75$ ksi*	
	Measured	Computed	Measured	Computed	Measured	Computed
1	2060	1870 (-9%)	2230	2030 (-9%)	2790	2660 (-5%)
2	1950	1670 (-14%)	2100	1840 (-12%)	2790	2400 (-14%)
3	2270	2050 (-10%)	2390	2230 (-7%)	2860	2910 (+2%)
4	1110	1180 (+6%)	1260	1280 (+2%)	2290	1670 (-27%)
5	2310	2910 (+26%)	2560	3160 (+23%)	3040	4130 (+36%)

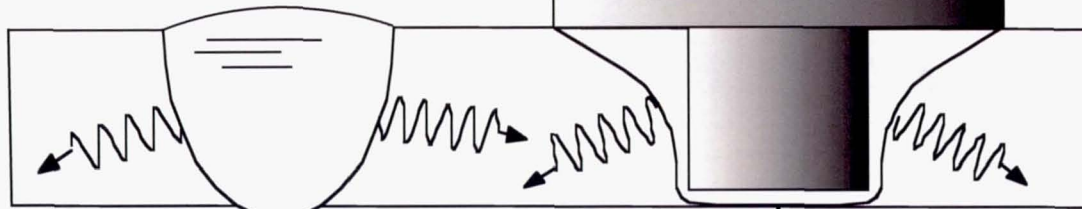
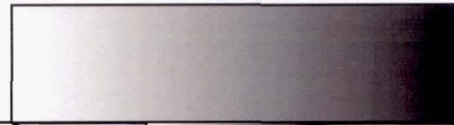
* Chosen for optimal data fit.

Power Requirements

Fusion Welding



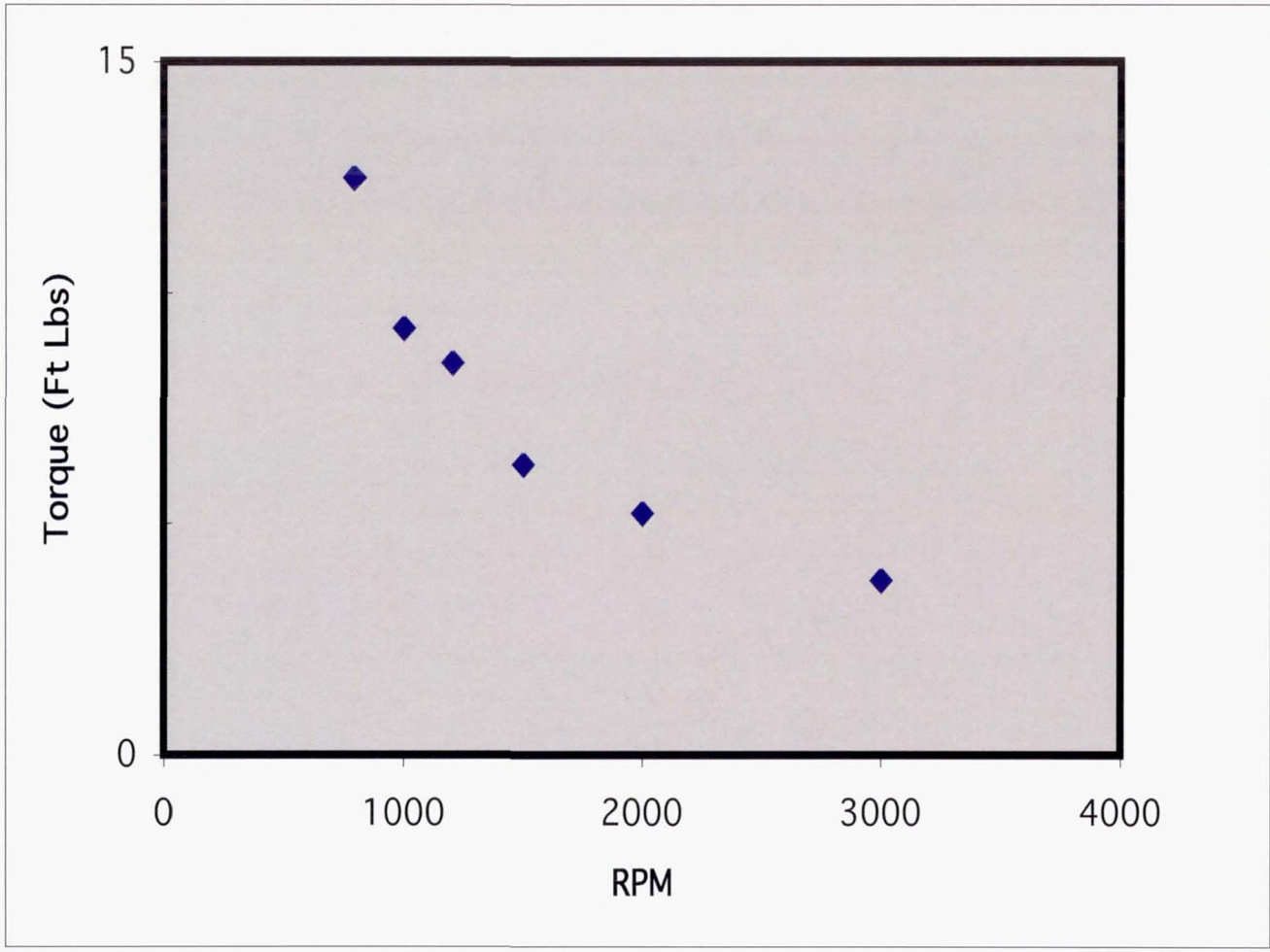
Friction Stir Welding



~ Melting
Temperature
at Melt Pool
Surface

~ 0.8 Melting
Temperature at
Shear Surface

Heat Losses of Fusion Welds and Friction Stir Welds Are Similar

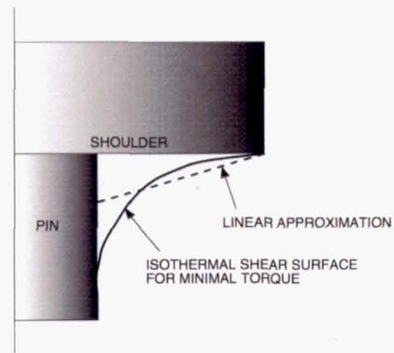


Courtesy of R. Carter/MSFC Metals Engineering Branch

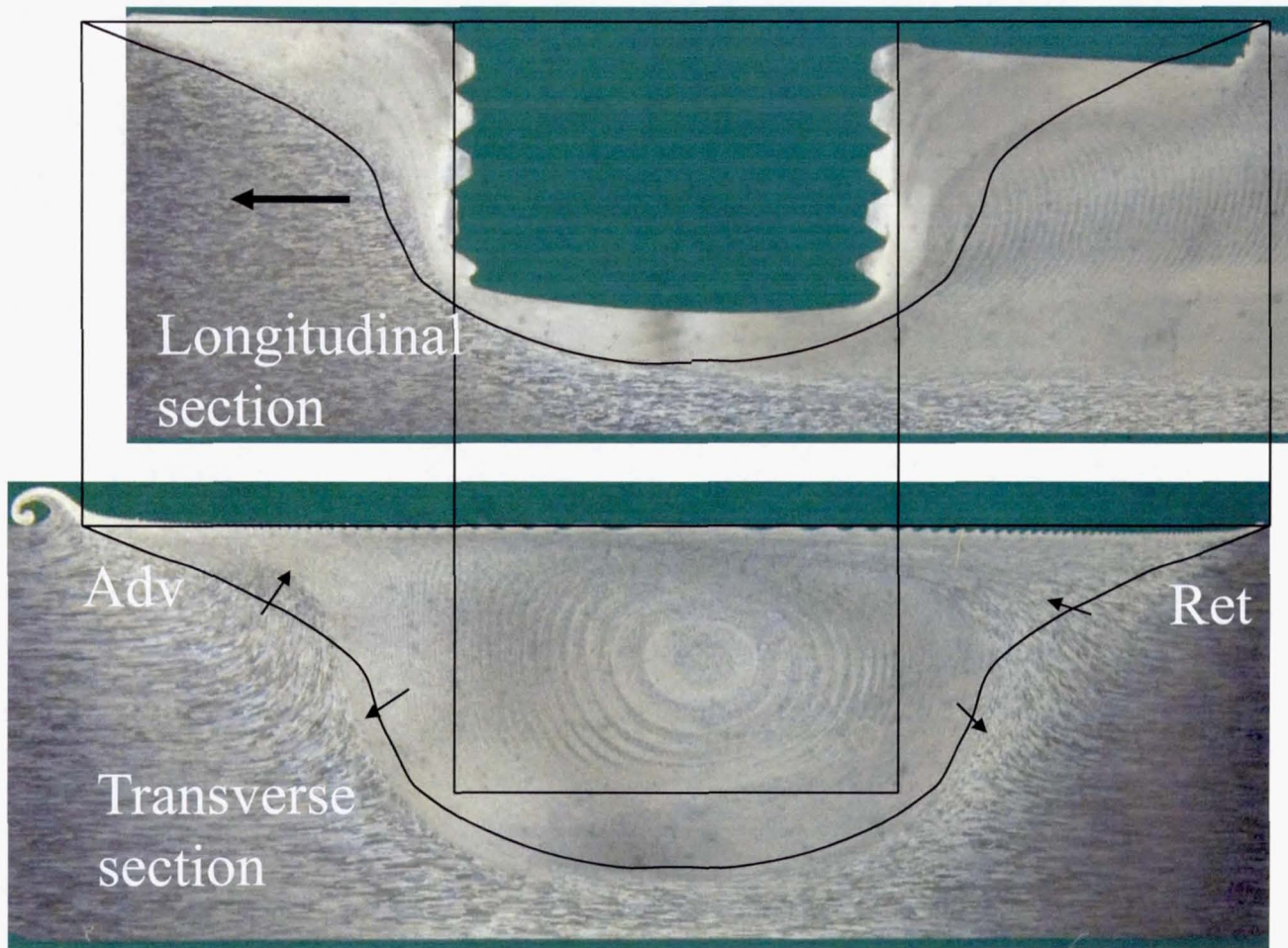
The Third Dimension

Minimization of torque (assuming constant t)

$$\delta \int_{\text{Shearing Surface}} 2\pi r^2 \tau \sqrt{1 + i^2} dz = 0 \quad \therefore z = aF(\varphi \setminus \alpha) \quad \varphi = \cos^{-1}\left(\frac{a}{r}\right) \quad \alpha = 45^\circ$$

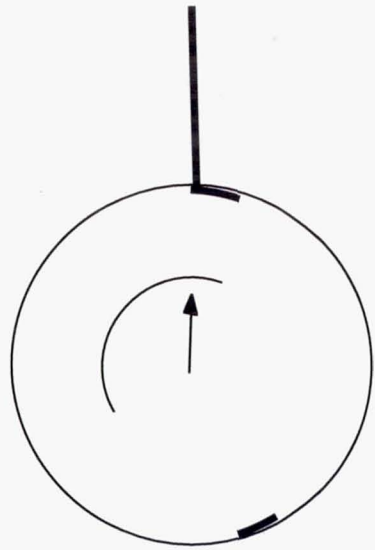


The computed shear surface shape (solid line) yielding minimal torque/power for isothermal/constant flow stress FSW tool environment. $F(\varphi/\alpha)$ is an elliptic integral of the first kind. A simplified linear approximation (dashed line) is also shown.

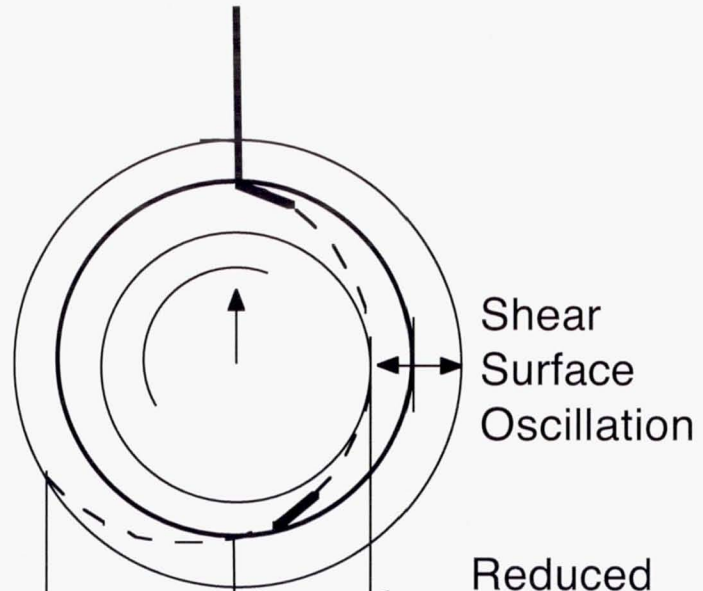


Courtesy of J. McClure/University of Texas at El Paso

Fragmentation

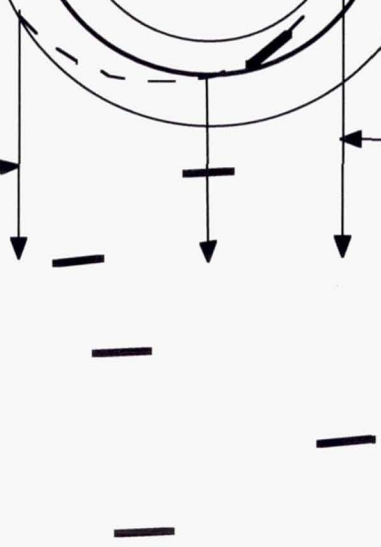


Scatter

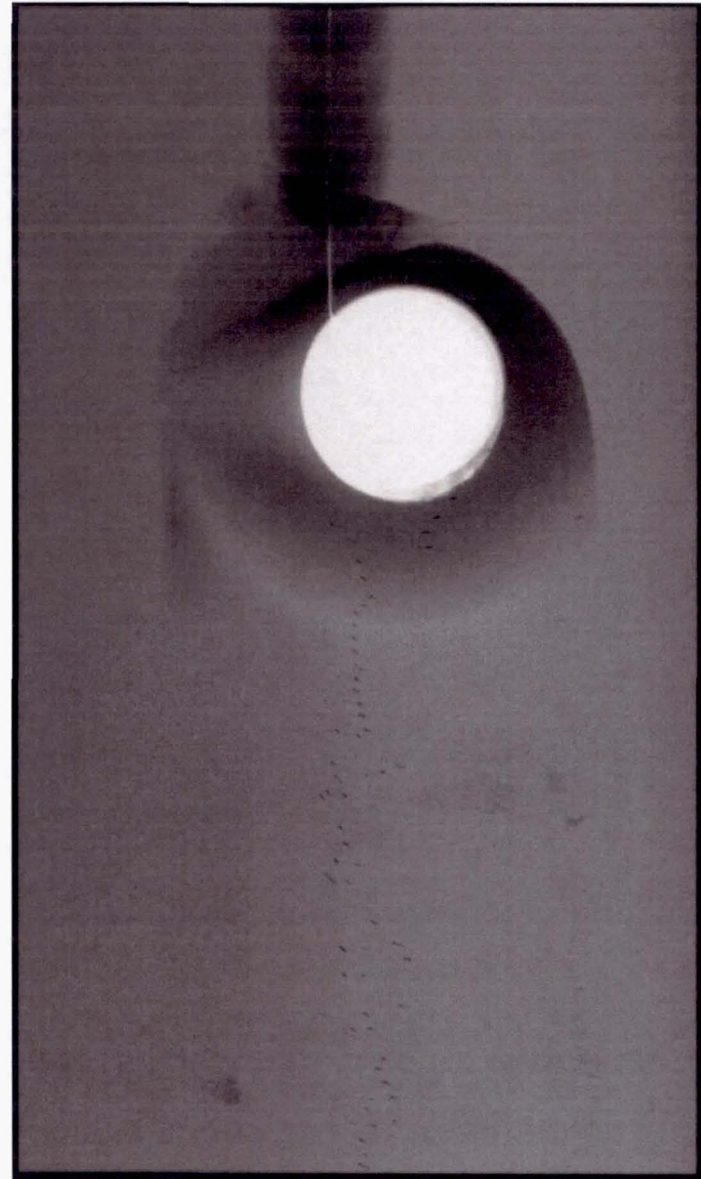
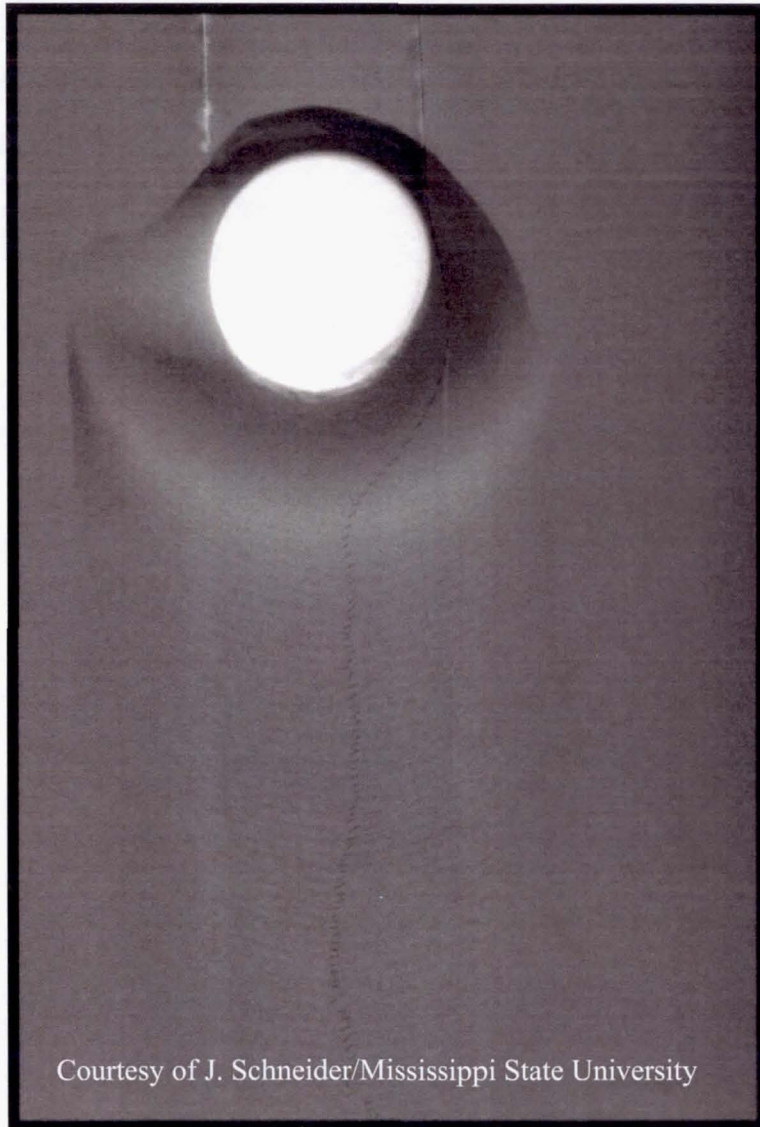


Expanded Radius

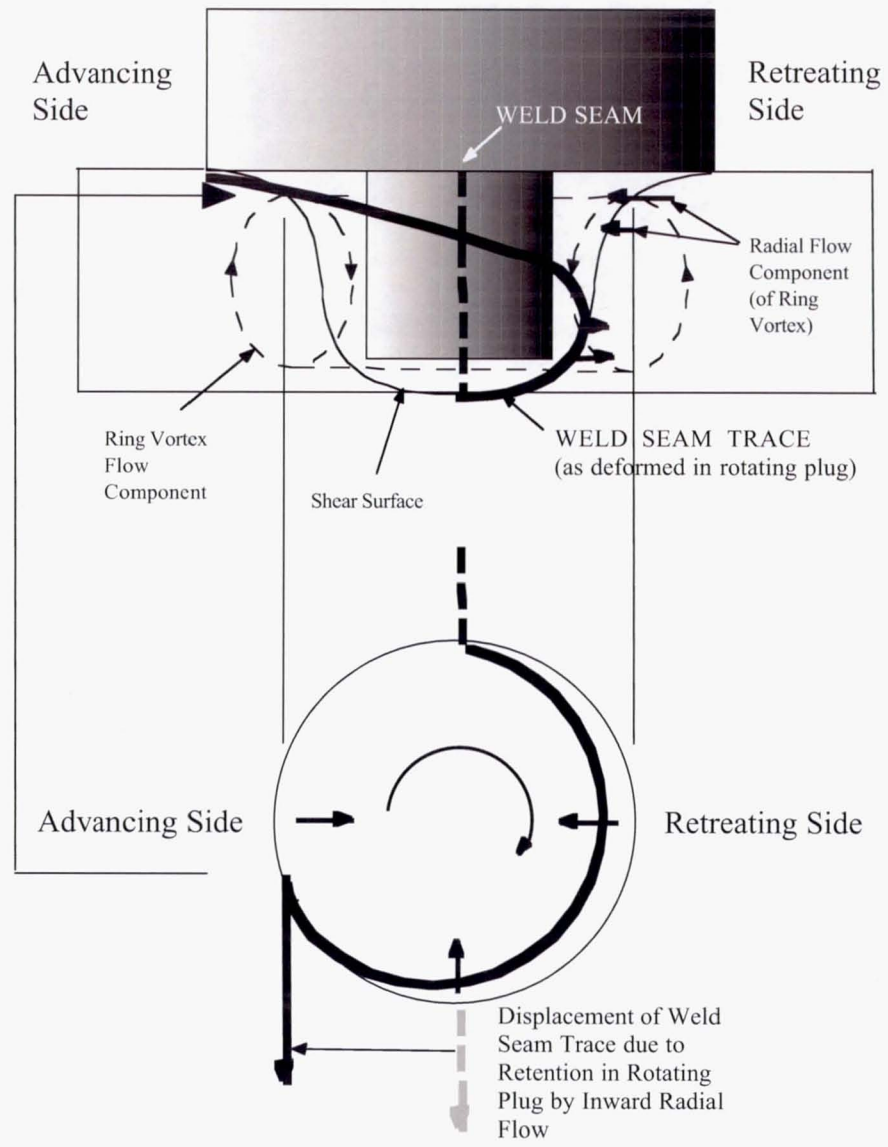
Reduced Radius



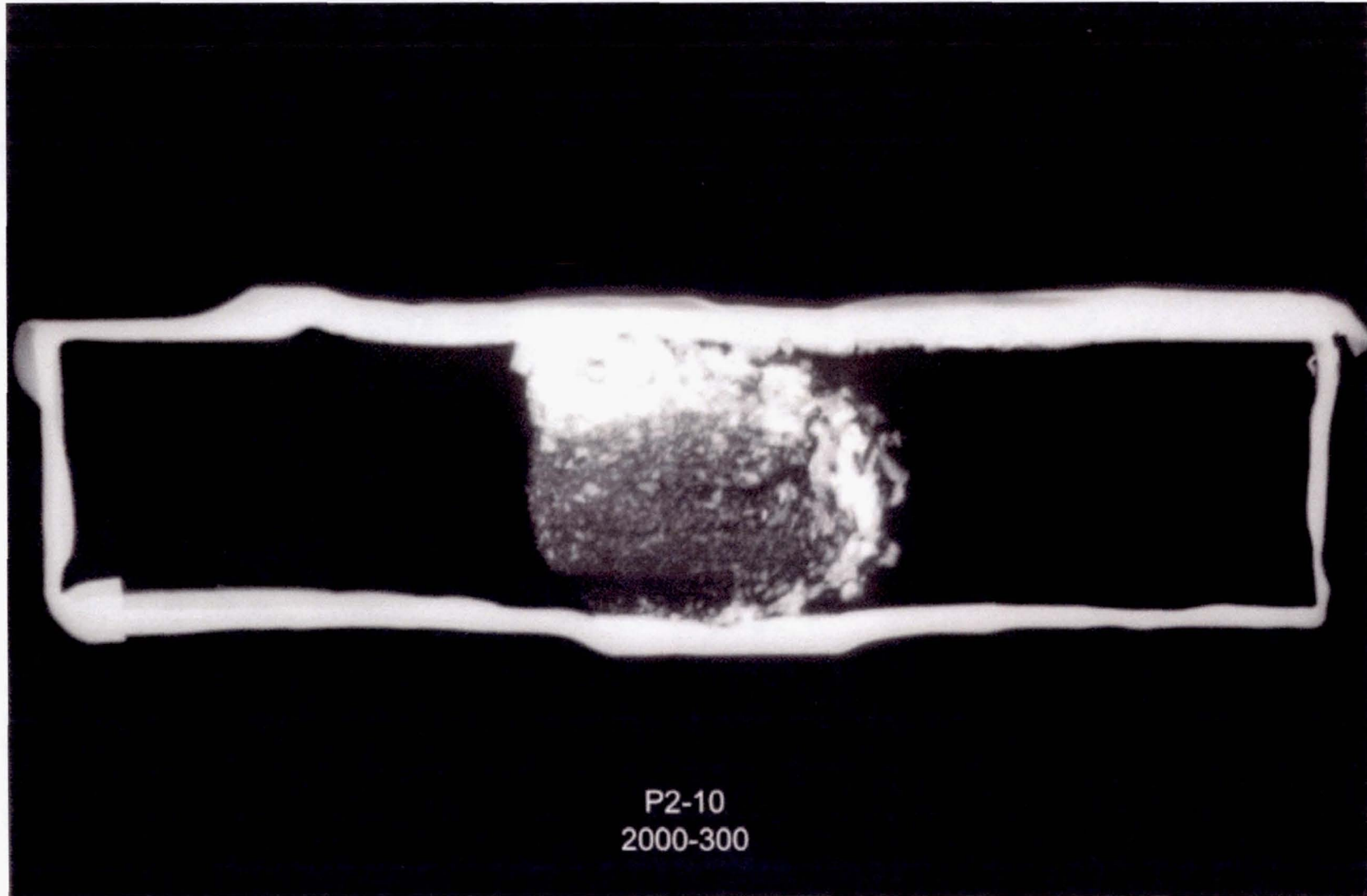
Radiographs of wire trace about FSW tool



Courtesy of J. Schneider/Mississippi State University



Tracer radiograph of displaced weld seam



Avoiding Defects

Defect causes

- **Parameters** (rpm, weld speed, plunge force):
flash, trenches, surface fissures, wormholes
- **Joint preparation** (e.g., seam cleanliness):
residual oxide defect
- **Tool design** (e.g., pin bottom-anvil clearance):
lack of penetration

CONCLUSION:

Control friction stir welds
using a kinematic model

- Weld structure controls weld properties.
- Weld flow field controls weld structure.
- **Specific aspects of weld process parameters and tool design control components of weld flow field (in kinematic model).**
- We control weld process parameters and tool design.